Croatian Society for Materials Protection

Metalurgija/Metallurgy

Vol. 65 No. 2 / 2026

Numerical Analysis of Shear Force for Oblique Edge Die-cutting Shear Utilizing ANSYS LS-DYNA

Dongfang Li [1]*, Mingliang Zheng [2]*,Zengyang Huang [3], Wentao Fu [4], Haibin Lin [4] and Sufen Wang [5]

https://doi.org/10.64486/m.65.2.1

[1] School of Mechanical and Electrical Engineering, Quzhou College of Technology, Quzhou 324000, China; ldf_keer@163.com
[2] School of Mechanical and Electrical Engineering, Huainan Normal University, Huainan, 232038, China; liangmingzheng@hnnu.edu.cn
[3] Quzhou Intellectual Property Protection Center, Quzhou 324000, China; 897581793@qq.com
[4] Quzhou Academy of Metrology and Quality Inspection, Quzhou 324000, China; 312887541@qq.com
[4] Quzhou Academy of Metrology and Quality Inspection, Quzhou 324000, China; linhaibin_zj@163.com
[5] College of Mechanical Engineering, Quzhou University, Quzhou 324000, China; wangsufen09@163.com
* Correspondence: Mingliang Zheng, liangmingzheng@hnnu.edu.cn
Dongfang Li, ldf_keer@163.com

Type of the Paper: Article
***Received*:** August 7, 2025
Accepted: October 15, 2025

Abstract: This paper presents the development of an advanced finite element model for predicting shear forces during the oblique-edge punching of Q235B steel, a material widely used in industrial applications. The model, developed in ANSYS/LS-DYNA, investigates the influence of key parameters such as shear edge inclination, strip thickness, punching depth, and lateral clearance. Results indicate that peak shear forces decrease significantly as the shear edge inclination increases from 4.0° to 4.8°. Furthermore, the optimal lateral clearance is found to be between 0.2 mm and 0.4 mm, leading to improved tool performance and material integrity. Model validation shows an error range of 8.47 % to 10.87 %, confirming its accuracy and practical applicability. This study offers valuable insights for optimizing tool design and enhancing punching efficiency in industrial settings, particularly in cold rolling mills. Future work will extend the model to a broader range of materials, incorporate advanced tool geometries, and account for thermal effects, thereby deepening the understanding of the shearing process and enabling further improvements in tool performance.

Keywords: shear force; oblique edge die-cutting shear; numerical simulation; ANSYS /LS-DYNA

1. Introduction

In the continuous rolling process line, the tail and head of the front and rear coil strips must be welded by special welding machines. Therefore, the welded strip joints need to be cut by punching shears, which facilitates the subsequent process of cutting feed and withdrawal functions of the disc shear. Hence, the accuracy of the slotting position on the edge of the punching shears directly impacts the edge-trimming effect of subsequent shearing equipment [1]. The strip undergoes elastoplastic deformation of the material up to the fractured state. Shear cutting, especially by means of oblique-edge punching tools, represents a very important process for

numerous industrial applications, ranging from metalworking to material fabrication. Accurate prediction of shear force is crucial for tool design optimization, reduction in tool wear, and material quality. Numerical simulations, particularly FEM, have considerably advanced understanding of the shearing process across a wide range of materials and conditions. Numerical simulation, notably FEA, has been at the forefront of material behavior predictions in processes related to metal cutting and shearing. Studies like that of Lawanwong et al. [2] on die wear and cycle capacity during blanking operations showed how FEA can compute tool wear and optimize the cutting process for different materials. This work highlighted the importance of modeling not only the shear force but also the degradation of tool surfaces over time, which significantly impacts production efficiency. Sontamino et al. [3] compared cut surface features in shearing, blanking, and punching processes. They found that blanking caused the most cracks, leading to the roughest surface, while punching produced the smoothest surface. Experimental results were corroborated by FEM simulations, and complex shapes necessitated an understanding of die-cutting parameters. Similarly, Moiceanu et al. [4] also modeled the shearing behavior of Miscanthus stems using FEA, studying the impact of different edge angles and cutting speeds on shear forces. These works illustrated the flexibility of FEA to simulate a wide variety of geometries and materials and provided critical insight into improving tool design and the process itself.

Accurate representation of material behavior in shear-cutting simulations, however, is quite important, and different material models have been developed to capture the complexities that arise when materials deform under stress. One of these is the Cowper-Symonds material model, one of the most sought-after strain-rate-sensitive material models, especially in high-speed cutting applications. This model accounts for both isotropic and kinematic hardening. It is thus well-suited to accurately capture the complex elastoplastic behavior of metals in dynamic loading conditions. Sontamino et al. [5] investigated the cut-surface features in die-cutting processes for thin and thick sheet metal parts using FEM simulations and experiments. The studies revealed that the proper choice of die-cutting clearance relative to material thickness is the decisive factor for optimum cut-surface quality. Furthermore, a fuzzy logic model was developed to assist in choosing the optimum clearance, and it proved quite effective. The results showed good agreement between the experimental findings and FEM simulations. Numerical simulations were also conducted using LS-DYNA and ANSYS Workbench in previous studies, such as those by Polat [6] and Groche et al. [7], on the punching and shearing process of several materials, including steel plates and spring sheets. These studies have validated material models such as Cowper-Symonds used in this work and have laid a foundation for understanding how material properties such as yield strength, strain rate sensitivity, and failure strain affect the shearing process. Zhang et al. [8] analyzed the effect of friction in the punching process using DEFORM software and found that the coefficient of friction has a significant influence on the force and shear quality. Friction between the upper and lower dies, affecting the shear process, was analyzed using numerical and experimental methods in other works by Kanyilmaz [9], Gomah and Demiral [10], by comparing a novel design of a punch with a hemispherical ball on the face, conducted experimentation and investigation on enhancements in blanking and piercing shearing processes. Using ABAQUS/Explicit finite element simulations with the Johnson-Cook material model, they identified topology optimization of the punch geometry. Wear resistance for TiN, CrN, TiSiN, AlCrN, and AlTiN-coated punches, as well as polycrystalline diamond compact (PDC) cutters, was evaluated by SEM micrographs after 1,000 strokes in a dry condition. In addition, the wear resistance and performance of the novel punch were better than those of PVD-coated punches. In this context, friction models like surface-to-surface contact models in ANSYS/LS-DYNA become crucial for realistic predictions of shear forces.

Features such as lubrication, tool wear, and surface roughness contribute to friction behavior, and their inclusion in the model is vital for achieving realistic results. Lu et al. [11] used FEM to study the punching process of electrical pure iron DT4E and discussed the strain, stress, and temperature distribution during punching. A comparison and detailed examination of punching clearance, speed, wear, and lubrication of the upper and lower dies were presented, and the factors influencing the characteristics of the punching port were expounded. The influence of tool geometry on shear force has been the subject of numerous studies. For example, Wang et al. [12] used FEA to investigate the effect of different shear edge designs on cutting force and tool wear in agricultural applications. They demonstrated how tool inclination, edge radius, and lateral clearance

 https://doi.org/10.64486/m.65.2.1

significantly influence shear force and material deformation. Similarly, Zafar et al. [13], explored how varying cutting-edge geometry affects the distribution of shear forces in Q235 steel, providing valuable insights for tool design optimization. Si and Gong [14] investigated the impact of 3D stress states and unloading rates on rockburst mechanisms by conducting triaxial unloading compression tests on fine-grained granite specimens. The results showed that higher confining pressures increase rock strength and energy accumulation, leading to more severe rockbursts. Lower unloading rates enhanced rock strength, allowing for the accumulation of more elastic energy. The failure mode transitioned from shear-tension to tension as confining pressure increased, indicating a significant weakening effect due to unloading. This research emphasizes the need for a 3D strength criterion to better understand rockburst mechanisms. Punched hole diameter, friction factor in the punching process, and punching speed were the factors that showed effects on the quality of the cross-section of the punching port. Agrawal et al. [15] established a punching process analysis model for thin metal strips using LS-DYNA analysis software and discussed the effects of punching shear edge clearance, edge overlap, and punching speed on the punching process. Although many research works have been conducted on the behavior of shear forces in straight-edge cutting, blanking, and punching, there remains a significant scientific gap in understanding the performance issues of oblique shear edges, especially in industrial applications involving thicker materials.

While straight-edge shearing has been well addressed in the literature, little has been said about the application of oblique-edge punches in terms of effectiveness in force distribution and tool wear reduction. Due to the lack of comprehensive numerical simulation studies of oblique shear edges, the optimization of such tools is incomplete, with major parameters such as cutting-edge inclination, strip thickness, and lateral clearance scarcely addressed. While existing research primarily deals with simple cutting geometries and thinner materials, the shear behavior of oblique-edge operations on thicker industrial metals has barely been explored. The present study seeks to fill these gaps by developing a detailed finite element model to analyze the shear behavior of oblique-edge punches, thereby optimizing the design parameters for industrial applications. It will also provide further insight into tool efficiency and longevity. To summarize, existing simulation studies have not yet addressed conditions involving non-entire circumferential edges, and what is referred to as the punching shear edge in the literature is specifically termed the oblique edge. Accordingly, this study investigates the punching process of oblique-edge punching shears and predicts the associated shear force using ANSYS/LS-DYNA software, with the aim of providing data support for optimizing structural design and process debugging of such shears.

2. Finite Element Modeling based on ANSYS/LS-DYNA

2.1. Modeling Assumptions

In developing the finite element model (FEM) that simulates the oblique-edge punching process, several major assumptions must be made to simplify material behavior and boundary conditions, while ensuring that the model is relevant to practice. One major assumption is the use of the Cowper-Symonds material model to simulate the elastoplasticity of Q235B steel, mainly under dynamic shear forces. This model assumes strain-rate dependence of material properties, which is important for shearing at high speeds; however, it does not consider the anisotropy or temperature effects that may occur during rapid cutting. Additionally, the upper and lower shear edges were modeled as rigid bodies. Because the contact interaction between the tool and material would be very complex, the computational load is reduced by simplifying this interaction. Although this assumption serves a practical purpose in many engineering applications, it may slightly underestimate tool wear or deformation effects with long-term usage. ANSYS APDL [16] is used for parametric modeling to model and solve the problem more conveniently. Figure 1 and Table 1 shows the simplified diagram of the punching shears.

https://doi.org/10.64486/m.65.2.1

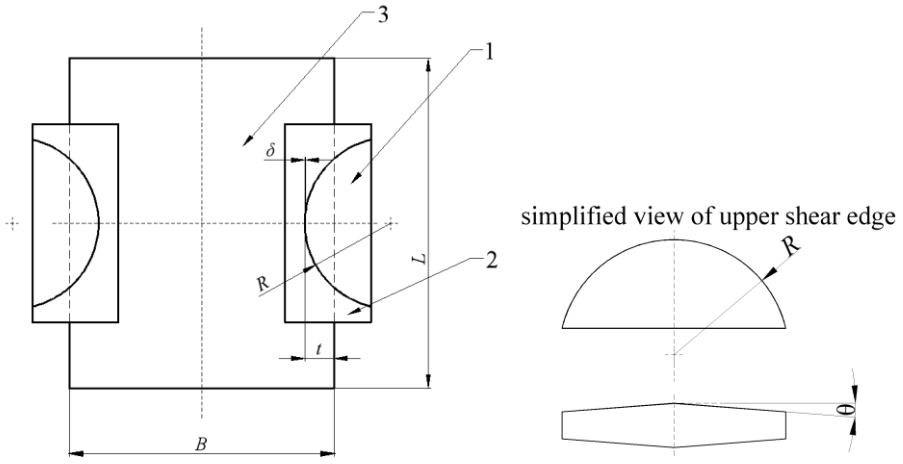

Figure 1. Simplified diagram of punching shears

Table 1. Main structural geometric parameters of punching shears

Parameter	Definition	Unit	Parameter	Definition	Unit
R	Upper and lower shear edge radius	mm	t	Punching and cutting depth	mm
B	Strip width	mm	L	Strip length of the model	mm
b	Strip thickness	mm	h	Strip thickness of the model	mm
δ	Lateral clearance of shear edge	mm	θ	Upper shear edge inclination	°

2.2 Mesh Sensitivity Analysis

The accuracy of Finite Element Method (FEM) results is highly sensitive to mesh refinement, particularly in regions near the shear edges where large deformations occur. In this study, a structured mesh was employed to refine the shear area, enabling a more accurate capture of material response during the two critical stages of cutting and fracture. The 3D solid element (element type 164 in LS-DYNA) within the explicit dynamic framework was utilized, which is well-suited for shear-dominated analyses. In general, two primary algorithms are available for dynamic analysis: single-point integration and full integration [16]. Given that the punching process involves large deformation and material failure, the single-point integration algorithm was adopted, with due consideration of the hourglass effect. A half-symmetric model was established based on both the geometric symmetry of the problem and computational constraints. The simplified numerical model includes three main components: the upper shear edge, the lower shear edge, and the strip. To evaluate the influence of mesh density, several lateral clearance ratios were tested—specifically, 1/3, 2/5, 1/2, 2/3, and 3/4 of the actual clearance. A mesh sensitivity analysis revealed that finer meshes yield more stable and accurate predictions of shear force and material deformation. However, this improvement in accuracy comes at the cost of increased computational time, highlighting a trade-off between numerical precision and computational efficiency. While refined mesh in the shear region showed that coarser meshes could predict general trends in shear force without capturing the stress concentrations and exact fracture mechanics, overly fine meshes would excessively increase computational demand with a disproportionate effect on improving the precision of the results. The final mesh density chosen was such that repeated testing created an optimal balance between accuracy and computational

https://doi.org/10.64486/m.65.2.1

efficiency, as evidenced by the mesh refinement producing results within an acceptable error range when compared to empirical data. The most stable solution was then selected from the modeling density and the shear model determined through repeated debugging in Figure 2.

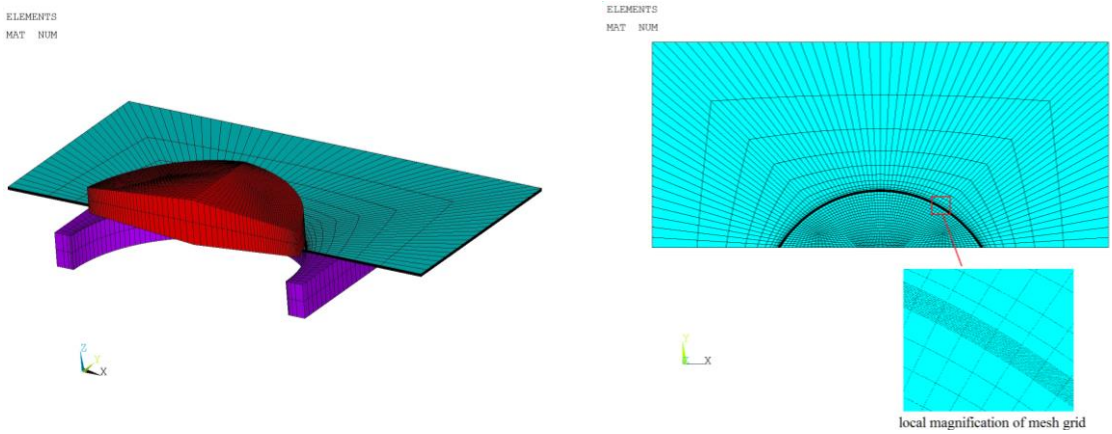

a) 3D view from the drive side b) Front view from the drive side

Figure 2. 3D finite element model and mesh refinement of shear region

2.3 Parametric Studies

In view of this, a systematic parametric study was performed in order to comprehensively understand the shear behavior during oblique-edge punching. This model studied several critical shear parameters, including the inclination of the upper shear edge θ, strip thickness h, punching depth t, and the lateral clearance δ between the shear edges. This numerical parametric study has been used to quantify the variation of each of these parameters with the resulting shear force and material deformation in general during the cutting process.

The outcomes showed that with an increased inclination angle of the upper shear edge, the peak shear force was reduced due to a more distributed cutting action. Inclinations in the range of 4.0° to 4.8° were established to provide the optimum compromise between minimum shear force and acceptable quality. Additionally, thicker strips needed higher shear forces (for example, 6 mm compared with 2 mm), with the shear force increasing with the square of the thickness of the strip because of the greater area of material being cut. The lateral clearance between the shear edges became another determining factor for the cutting force, while the optimal clearances for a clean cut and without excessive tool wear or material deformation were identified within a range from 0.2 mm to 0.4 mm.

In summary, the parametric study underlined complicated interactions between these parameters, which developed a design to be cautious about achieving minimal shear force while optimizing tool performance and material integrity. The results provide valuable insights that can be used to guide the design of oblique-edge punching tools in industrial applications, offering a data-driven approach to improving efficiency and reducing tool wear.

2.4 Material Model

The strip material is Q235B steel [17]. At room temperature (20 °C), the material constants are as follows: elastic modulus (E) is 2.03×10^5 MPa, Poisson's ratio (μ) is 0.3, density (ρ) is 7850 kg/m^3, yield stress (σ_Y) is 235 MPa, tangent modulus (E_{tan}) is 791 MPa, tensile strength (σ_b) is 375 MPa, and failure strain (ε_f) is 0.34.

The material strip follows the Cowper-Symonds model [16], [17] set as a mixture model for kinematic hardening, isotropic, or hybrid of the two and related to the strain rate. The hardening parameter of the model is set to 1, and the strain rate and coefficient are set to 0. Then, both the upper and lower shear edges were selected as rigid models, and their density, elastic modulus, and Poisson's ratio are assigned as 7850 kg/m^3, 210 GPa, and 0.3, respectively. The shear edge radius R used in the model of this paper is taken as 260 mm.

https://doi.org/10.64486/m.65.2.1

2.5 Boundary Conditions

The contact of the strip with the upper and lower shear edges is defined as rigid body-deformation body automatic surface-to-surface contact (ASTS). Additionally, the friction coefficient is a crucial parameter affecting contact interactions. The static and dynamic friction coefficients between steel surfaces are set to 0.15 and 0.1, respectively. Considering the punching process, the stress condition of the model is that the lower shear edge is fully constrained, and the upper shear edge is restricted only to vertical downward motion (RBVZ) as defined in APDL, with symmetric constraints applied to the strip. Regarding the setting of solution time, the whole process of punching is simulated, including the time taken by the upper shear edge to completely shear. For instance, at a shear speed of 92.4 mm/s, the total calculation time will be roughly 0.2 seconds.

3. Model Verification

3.1. Calculation Method of Sheer Force of the Circular Shear Edge

The shearing angle (α) is calculated using the shear edge drawing method. The shearing angle (α) is determined by the formula:

$$\alpha = \arctan(2\Delta t/l) \tag{1}$$

Where Δt represents the thickness variation and l is the length.

The calculation formula[13] for the Kololov sheer force of the shears with an oblique edge, considering the lateral clearance coefficient K_1 and the blunt coefficient K_3 of the shear edge, is expressed as:

$$F = (0.7\sim0.75)K_1K_3\frac{2-\varepsilon}{2\tan\alpha}\varepsilon h^2\sigma_Y \tag{2}$$

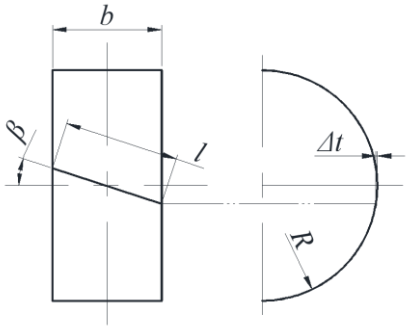

Figure 3. Plane graph of the formation of the shear edge

Figure 3 illustrates the plane graph of the formation of the shear edge, offering a detailed depiction of how the shear edge interacts with the material during the cutting process. This diagram serves as a crucial visual aid in understanding the geometric relationship between key parameters, such as the radius of the shear edge, the projected height difference Δt, and the projected length l. It highlights how these parameters contribute to the overall shear angle α, which in turn influences the distribution of forces along the shear edge.

3.2 Reliability Verification of Punching and Cutting Model

Shear force is the fundamental dynamic parameter for designing the detailed structure of punching shears. The precision, which comes from model operations, is closely related to the rational establishment of the model. This section focuses on the shear model of a flat shear edge, whose different punching and shearing depths were set at 40 mm, 80 mm, and 125 mm, respectively, in analyzing and verification under the following conditions: thickness 6.0 mm, width 450 mm, shear edge clearance 0.3 mm, shear velocity 92.4 mm/s, and upper shear edge inclination angle θ = 0°. Numerical results are compared to the empirical formula outcomes [2], listed in Table 2.

https://doi.org/10.64486/m.65.2.1

Table 2. Comparison of numerical results and outcomes of the empirical formula

No.	Cutting depth / mm	Literature solution / kN	Numerical solution / kN	Error / %
1	40	394.6	351.7	10.87
2	80	565.9	510.6	9.77
3	125	719.4	658.5	8.47

3.3 Reliability Verification of Punching, Cutting, and Cutting Model

Table 2 depicts that the error between the numerical solution and the findings presented in the literature related to the punching shear forces with cutting depths of 40 mm, 80 mm, and 125 mm is between 8.47 % and 10.87 % when the condition of the flat shear edge is considered. However, it should be noted that the above results are obtained under the assumption of the flat shear edge, and the shear model has been appropriately simplified, so the results are only approximations. The effects of factors such as the lateral clearance of the shear edge and the friction between the sheet metal and the upper and lower shear edges in the punching process are omitted. Nevertheless, the operation results can indeed meet the actual needs of the project to a certain extent. Therefore, the above errors are acceptable in engineering applications. In addition, the distribution trend of the sheer force of the flat shear edge under different cutting depth values is roughly the same, as can be observed in the curve of the punching shear force curve shown in Figure 4. To sum up, the punching and cutting model constructed in the manuscript is reliable.

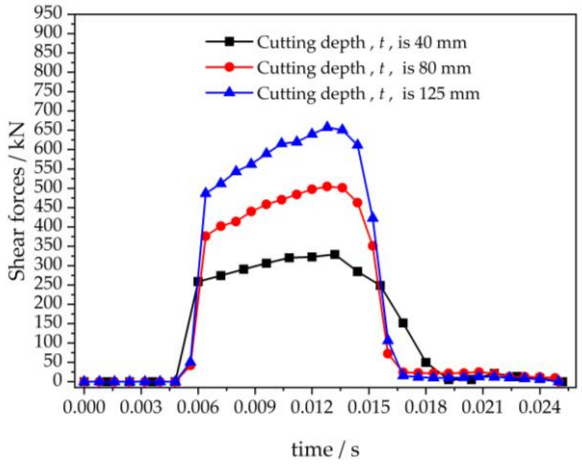

a) Time history curve of shear force at different *t* b) *t* is the punching after shearing of 80 mm

Figure 4. Time history curve of shear force and punching after shearing of flat shear edge with different *t*

4. Analysis and Results

The inclination angle of the upper shear edge was set to 4.4° in this section unless otherwise indicated, and the lateral clearance between the upper and lower shear edges was kept at 0.3 mm unless otherwise indicated. Using the orthogonal experiment method, the shear rate in the experiment was set to 92.4 mm/s. Given different punching depths, strip thicknesses, and lateral clearances of the shear edge, the distribution of the shear force for the strip is pursued in great detail.

4.1 Analysis of the Punching Process of the Punching Shears

The model parameters in this section are defined as follows: the length L= 1000 mm, the width B = 900 mm, the thickness h= 6 mm, and the lateral clearance of the shear edge δ = 0.3 mm. The main motion involves the vertical linear movement of the upper shear edge at a speed of 92.4 mm/s. To analyze and visually observe the strip shearing process until fracture, the upper and lower shear edges are hidden in this analysis, showing only

https://doi.org/10.64486/m.65.2.1

the strip model. The equivalent stress nephogram of the Von Mises node is then extracted for visualization. The cloud nephogram illustrating the strip punching process is presented in Figure 5.

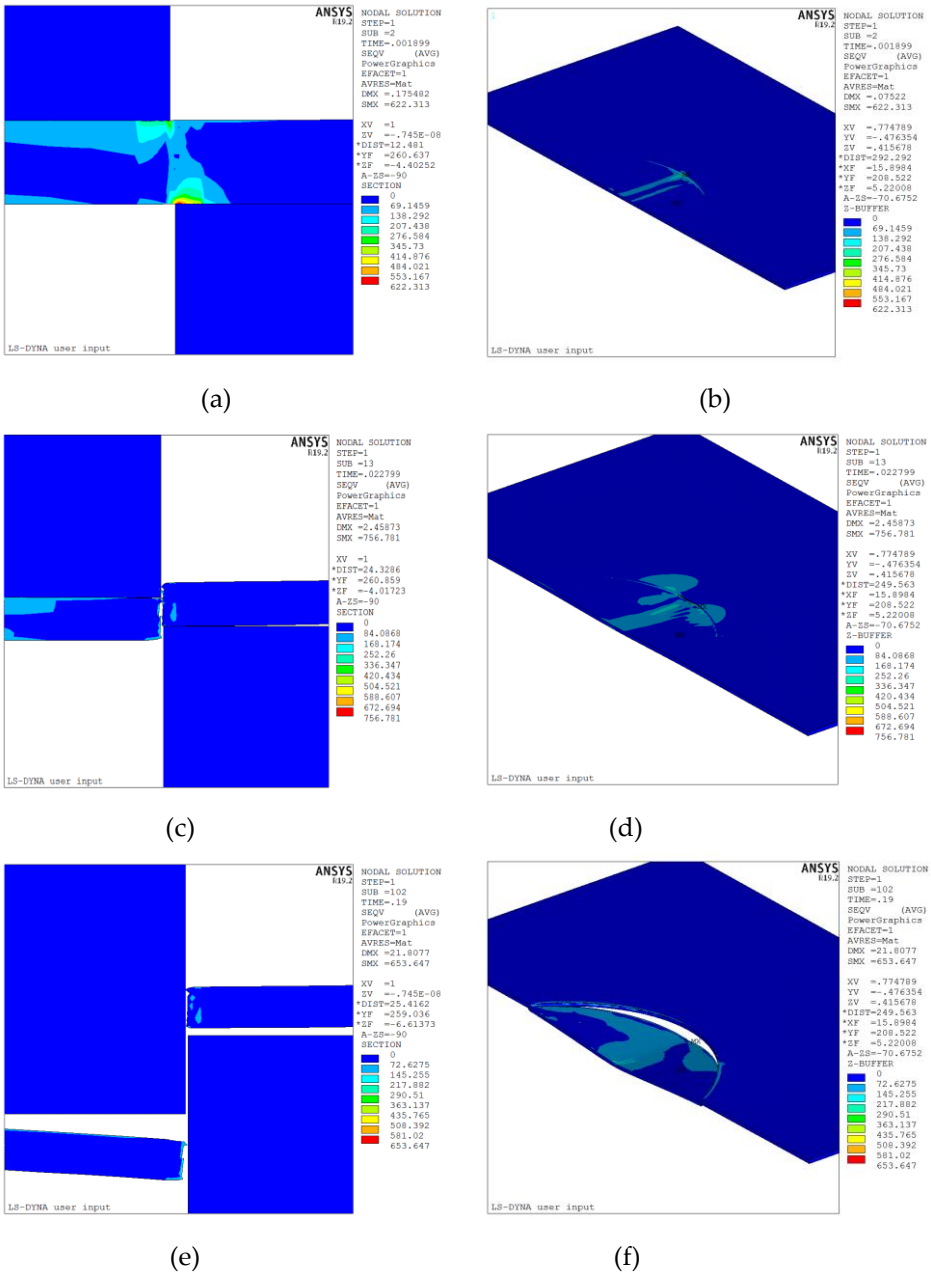

Figure 5. Stress cloud nephogram of strip punching process

In Figure 5a, at the simulation time of 0.01899 s, the upper shear edge moves in the shearing direction, and the maximum Mises stress reaches 622.313 MPa, exceeding the limit strength of the strip, so the strip element fails. In figure 5b, the node of the maximum stress generated on the strip is at the location marked by "MX". In Figure 5c, at 0.022799 s, the upper shear edge keeps moving until all the elements of the middle cross-section of the strip completely fail, leading to fracture. In Figure 5d, the fracture pattern of the strip exhibits an "arc of the shear edge that rapidly expands to the edge of the strip" during the 13th step of the simulation. In Figure 5e and 5f, both show the simulation at the 102nd step, at an analysis time of 0.19 s when the strip is completely punched out along the arc direction.

https://doi.org/10.64486/m.65.2.1

4.2 Shear Force Distribution Under Different Inclinations of Upper Shear Edge

A punching model with a thickness of h = 6 mm, width B = 900 mm, length L = 1000 mm, and punching and cutting depth t = 125 mm was selected for consideration. The shear forces at different upper shear edge inclinations θ of 4.0°, 4.4°, and 4.8° were analyzed. Under the same model specifications, the maximum shear forces for inclinations of 4.0°, 4.4°, and 4.8° were 52.2 kN, 48.8 kN, and 51.1 kN respectively, shown in Figure 6; these represent relative errors ranging from 4.7 % to 7.0 %. During the entire steady punching process, the three values of shear force were approximately 36.2 kN, 35 kN, and 36.1 kN, respectively. The relative errors between them were about 3.1 %~3.5 %. Additionally, the distribution pattern of the shear force is similar, which shows that when θ is equal to 4.4°, the shear force is relatively stable. Therefore, this inclination can be regarded as the initial value of structural design.

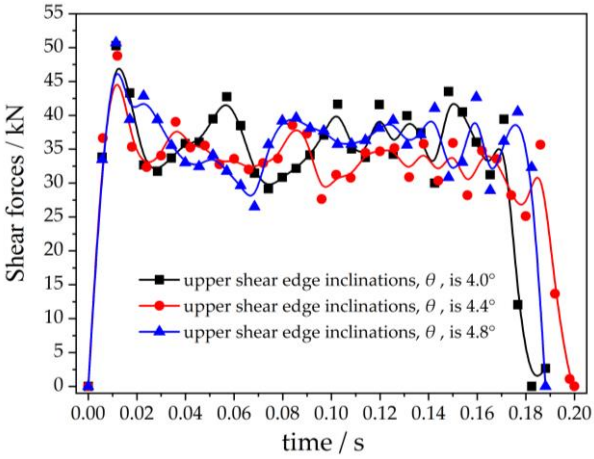

Figure 6. Distribution curve of shear force with time under different upper shear edge inclinations

4.3 Shear Force Distribution Under Different Punching and Cutting Depths

The punching model that was chosen had the following dimensions: thickness h = 6 mm, width B = 900 mm, and length L = 1000 mm. Shear forces were researched at punching and cutting depths t of 125 mm, 80 mm, and 40 mm, respectively. According to Figure 7, when cutting depths are 125 mm, 80 mm, and 40 mm, respectively, under the same model specification conditions, the maximum shearing forces are 48.8 kN, 46.3 kN, and 43.7 kN, respectively, and the shearing forces in the steady punching process are about 35 kN, 30 kN and 25 kN respectively. The distribution rule of the shearing force is similar. As the shear area is also larger under greater punching and cutting depths, it increases with the increase of punching and cutting depth; correspondingly, the impact of the shear force would also become greater.

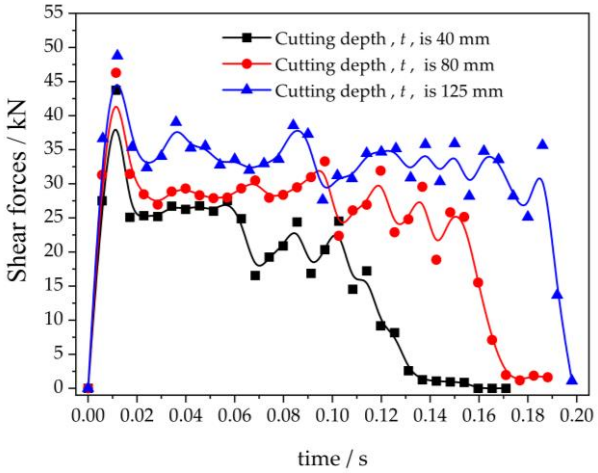

Figure 7. Distribution curve of shear force with time under different punching and cutting depths

https://doi.org/10.64486/m.65.2.1

4.4 Influence of Strip Thickness on Shear Force

Models of variable thicknesses of 2 mm, 4 mm, and 6 mm, with width B = 900 mm and length L = 1000 mm, were selected for a punching and cutting depth of t = 125 mm. As seen in Figure 8, under the same model condition, when the strip thicknesses are 2 mm, 4 mm, and 6 mm, their maximum shear forces will be 11.8 kN, 25.1 kN, and 48.8 kN, respectively. The shear forces are approximately 7.5 kN, 20 kN, and 35 kN, respectively, in the steady punching process. As the strip thickness increases, the corresponding shear area also grows larger, resulting in a higher shear force required to cut the strip.

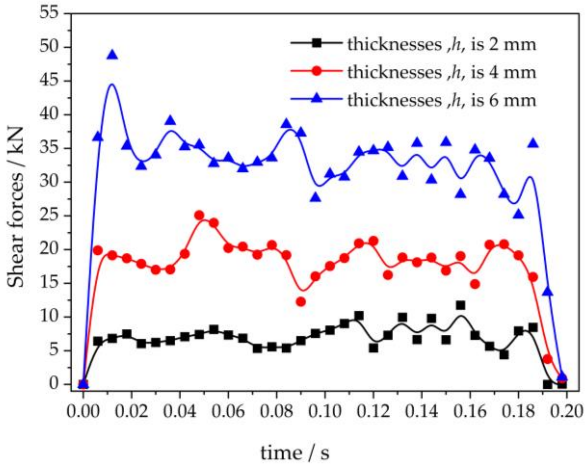

Figure 8. Distribution curve of shear force with time under different thicknesses

4.5 Influence of lateral clearance of shear edge on shear force

A model with a thickness of 6 mm, a width of 900 mm, and a length of 1000 mm was chosen, while the depth for punching and cutting was 125 mm. Under the same model specifications, the maximum shear forces for lateral clearances of 0.2 mm, 0.3 mm, and 0.4 mm were, respectively, 42.2 kN, 48.8 kN, and 52.9 kN, as illustrated in Figure 9. During the steady punching process, the shear forces were approximately 30 kN, 35 kN, and 40 kN, respectively. Quantitatively, the shear force distribution was close to each other among the different lateral clearances, with relatively stable changes during the whole punching process. More importantly, the oblique upper shear edge remarkably reduced the needed shear force. In all, an appropriate choice should be made for the lateral clearance of the shear edge. If too large, it would be difficult to cut the strip; if too small, collision or interference may occur on the shear edge, requiring higher assembly accuracy. The right lateral clearance of the shear edge should be chosen. Based on the former analysis, the best lateral clearance in this design may be within a range from 0.2 mm to 0.4 mm.

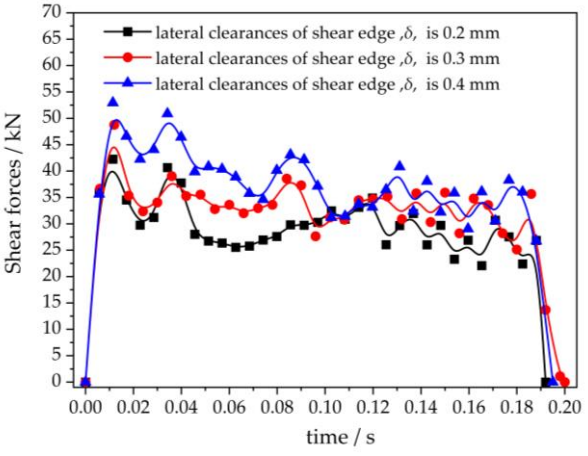

Figure 9. Distribution curve of shear force with time under different lateral clearances of shear edge

https://doi.org/10.64486/m.65.2.1

5. Discussion

Through a detailed analysis of shear force distribution under multiple influencing factors, the validity of the proposed model has been verified. Key parameters investigated include cutting-edge inclination, strip thickness, punching depth, and lateral clearance of the cutting edge. By systematically varying these parameters and comparing model predictions with expected results, the accuracy of the model has been confirmed.

Furthermore, it has been established that the maximum applicable strip thickness for shearing is 6 mm. Under conditions of smooth cutting and stable punching operations, the maximum recorded shear forces were 52.9 kN and 48.8 kN, respectively. These results indicate that strip thickness exerts a direct influence on the required shear force. In addition, lateral clearance of the cutting edge is identified as a critical factor in maintaining effective shearing performance. To ensure both smooth and efficient punching, a lateral clearance between 0.2 mm and 0.4 mm is recommended. Within this range, consistent shearing can be achieved without inducing excessive material resistance or tool interference. Deviations outside this range may lead to reduced cutting efficiency if the clearance is too large, or increased tool wear and potential failure if too small.

The influence of the upper cutting-edge inclination was also examined across a range of 4.0° to 4.8°. The results indicate that the shear force remains nearly constant when the inclination angle is set at 4.4° This value is therefore suggested as a reliable initial setting in structural design, as it offers an optimal balance between the required shear force and material behavior during punching.

Finally, the relationship between punching depth and shear force was analyzed. As punching depth increases, the shear area expands, leading to a corresponding rise in the required shear force. This is attributed to the greater volume of material being deformed in deeper punching operations. It should be noted, however, that although shear force escalates with depth, this also intensifies the mechanical demands on both the workpiece and the tool, potentially accelerating wear on the cutting edge over prolonged use.

6. Conclusion

This study provides valuable insights into the shear force behavior of oblique-edge punching tools, with several practical implications for industrial applications. The finite element model developed offers a reliable framework for predicting shear forces under various conditions, including shear edge inclination, material thickness, punching depth, and lateral clearance. Key findings reveal that a shear edge inclination between 4.0° and 4.8° enables more effective cutting without material detachment caused by peak shear forces. Additionally, optimizing the lateral clearance within the range of 0.2 mm–0.4 mm resulted in clean cuts and minimal tool wear. These insights provide actionable recommendations for the design of punching tools in industrial settings, particularly in cold rolling mills where tool wear and cutting efficiency are critical.

The significant contributions of this paper include the development and validation of a detailed finite element model for oblique-edge punching, the identification of optimal geometric parameters that minimize shear force, and a demonstration of how material properties, such as thickness and yield strength affect the shearing process. The model was validated using empirical data, with an acceptable error margin of 8.47 %–10.87 %, confirming its accuracy and applicability in real-world engineering scenarios.

Several promising directions for future research are identified. First, exploring other materials, such as aluminum, copper, and high-strength alloys, could further validate the model for a broader range of industrial applications. Another avenue involves incorporating thermal coupling into the model to better understand how heat generation during high-speed shearing influences material behavior and tool wear. Finally, future studies could investigate more complex tool geometries or the effects of prolonged tool wear by integrating dynamic boundary conditions for more realistic simulation of actual operating conditions. Since the current model does not account for strain rate effects or thermal softening, its ability to predict tool wear in high-speed punching remains limited. Thus, a critical next step is the incorporation of thermomechanical coupling.

https://doi.org/10.64486/m.65.2.1

Funding

The research is supported by: Science and Technology Research Key Competitive Project of Quzhou Science and Technology Bureau (No. 2023K266), General Research Project of Zhejiang Provincial Department of Education (No. Y202455816), Zhejiang University domestic visiting Engineers "School-Enterprise Cooperation Project" (No. FG2020219), Quzhou College of Technology School-level Science and Technology Innovation team (No. XKCTD202206), Quzhou College of Technology New School-level Research Institute (Center) Project (No. QZYJS202107).

References

[1] F. Avila Aparicio, *Broken Edge: Influence of Edge Trimming over Flat Rolled Steel in Hot Strip Mills*, M.S. thesis, Instituto Tecnológico y de Estudios Superiores de Monterrey, Monterrey, Mexico, 2007.

[2] K. Lawanwong and W. Pumchan, "Wear mechanism and ability for recovery of tool steel on blanking die process," *Key Engineering Materials*, vol. 725, pp. 572–577, 2016, https://doi.org/10.4028/www.scientific.net/KEM.725.572

[3] A. Sontamino and S. Thipprakmas, "Cut surface features in various die-cutting processes," *Key Engineering Materials*, vol. 719, pp. 127–131, 2017, https://doi.org/10.4028/www.scientific.net/KEM.719.127

[4] G. Moiceanu, P. Voicu, G. Paraschiv, and G. Voicu, "Behaviour of Miscanthus at cutting shear with straight knives with different edge angles," *Environmental Engineering and Management Journal*, vol. 16, no. 5, pp. 1203–1209, 2017, https://doi.org/10.30638/eemj.2017.126

[5] A. Sontamino and C. Nitnara, "A fuzzy logic base for selecting optimal clearance of die-cutting process," in *Global Congress on Manufacturing and Management*, vol. 335, pp. 157–168, 2021, https://doi.org/10.1007/978-3-030-90532-3_13

[6] E. Polat, "Investigation of concrete filled composite plate shear walls using finite element methods," *Uludağ Üniversitesi Mühendislik Fakültesi Dergisi*, vol. 25, no. 1, pp. 139–152, 2020, https://doi.org/10.17482/uumfd.621362

[7] P. Groche, S. Köler, and S. Kern, "Stamping of stringer sheets," *Journal of Manufacturing Processes*, vol. 36, pp. 319–329, 2018, https://doi.org/10.1016/j.jmapro.2018.10.025

[8] Y. Zhang, X. He, Y. Wang, Y. Lu, F. Gu, and A. Ball, "Study on failure mechanism of mechanical clinching in aluminium sheet materials," *The International Journal of Advanced Manufacturing Technology*, vol. 96, pp. 3057–3068, 2018, https://doi.org/10.1007/s00170-018-1734-2

[9] A. Kanyilmaz, "The problematic nature of steel hollow section joint fabrication, and a remedy using laser cutting technology: A review of research, applications, opportunities," *Engineering Structures*, vol. 183, pp. 1027–1048, 2019, https://doi.org/10.1016/j.engstruct.2018.12.080

[10] M. Gomah and M. Demiral, "An experimental and numerical investigation of an improved shearing process with different punch characteristics," *Strojniški vestnik – Journal of Mechanical Engineering*, vol. 66, no. 6, pp. 375–384, 2020, https://doi.org/10.5545/sv-jme.2020.6583

[11] Q. Lu, Y. Yao, J. Shi, Y. Shen, X. Huang, and Y. Fang, "Design and performance investigation of novel linear switched flux PM machines," *IEEE Transactions on Industry Applications*, vol. 53, no. 5, pp. 4590–4602, 2017, https://doi.org/10.1109/TIA.2017.2714998

[12] T. Wang et al., "Finite element model construction and cutting parameter calibration of wild chrysanthemum stem," *Agriculture*, vol. 12, no. 6, p. 894, 2022, https://doi.org/10.3390/agriculture12060894

[13] R. Zafar, L. Lang, and R. Zhang, "Experimental and numerical evaluation of multilayer sheet forming process parameters for lightweight structures using innovative methodology," *International Journal of Material Forming*, vol. 9, no. 1, pp. 35–47, 2016, https://doi.org/10.1007/s12289-014-1198-3

[14] X. Si and F. Gong, "Strength-weakening effect and shear-tension failure mode transformation mechanism of rock-burst for fine-grained granite under triaxial unloading compression," *International Journal of Rock Mechanics and Mining Sciences*, vol. 131, p. 104347, 2020, https://doi.org/10.1016/j.ijrmms.2020.104347

[15] P. Agrawal, S. Aggarwal, N. Banthia, U. S. Singh, A. Kalia, and A. Pesin, "A comprehensive review on incremental deformation in rolling processes," *Journal of Engineering and Applied Science*, vol. 69, no. 20, pp. 1–28, 2022, https://doi.org/10.1186/s44147-022-00072-w

[16] T. Zhang, *ANSYS APDL Parametric Finite Element Analysis Technology and Its Application*. Beijing, China: China Water Power Press, 2013 (In Chinese).

[17] H. Zhang, R. Hu, and S. Kang, *ANSYS 14.5/LS-DYNA Nonlinear Finite Element Analysis Example Guidance Tutorial*. Beijing, China: Machine Press, 2013, (In Chinese).

https://doi.org/10.64486/m.65.2.1